The Astrophysical Journal, 835:158 (5pp), 2017 February 1 doi:10.3847/1538-4357/835/2/158

Association of Plages with Sunspots: A Multi-Wavelength Study Using Kodaikanal Ca II K and Greenwich Sunspot Area Data

Sudip Mandal[1], Subhamoy Chatterjee[1], and Dipankar Banerjee[1,2]
[1] Indian Institute of Astrophysics, Koramangala, Bangalore 560034, India; sudip@iiap.res.in
[2] Center of Excellence in Space Sciences India, IISER Kolkata, Mohanpur 741246, West Bengal, India
Received 2016 November 25; revised 2016 December 16; accepted 2016 December 16; published 2017 January 25

Abstract

Plages are the magnetically active chromospheric structures prominently visible in the Ca II K line (3933.67 Å). A plage may or may not be associated with a sunspot, which is a magnetic structure visible in the solar photosphere. In this study we explore this aspect of association of plages with sunspots using the newly digitized Kodaikanal Ca II K plage data and the Greenwich sunspot area data. Instead of using the plage index or fractional plage area and its comparison with the sunspot number, we use, to our knowledge for the first time, the individual plage areas and compare them with the sunspot area time series. Our analysis shows that these two structures, formed in two different layers, are highly correlated with each other on a timescale comparable to the solar cycle. The area and the latitudinal distributions of plages are also similar to those of sunspots. Different area thresholdings on the "butterfly diagram" reveal that plages of area $\geqslant 4$ arcmin^2 are mostly associated with a sunspot in the photosphere. Apart from this, we found that the cyclic properties change when plages of different sizes are considered separately. These results may help us to better understand the generation and evolution of the magnetic structures in different layers of the solar atmosphere.

Key words: sunspots – Sun: activity – Sun: oscillations

1. Introduction

The Sun is a magnetically active star with a dynamic atmosphere that varies on a timescale from seconds to years. Different solar features are basically manifestations of the magnetic concentrations in different layers of the Sun. Plages are the chromospheric features that appear as bright patches on the solar disk when seen through Ca II K line (3933.67 Å) images, whereas sunspots are the dark photospheric features prominently visible in white-light images. Sunspots and plages both vary periodically on an 11 year timescale known as the "solar cycle." Apart from that, plages are found to be highly correlated with the location of the magnetic field concentrations (Sheeley et al. 2011; Chatterjee et al. 2016), very similar to sunspots.

Satellite measurements over the past few decades have revealed that the changes in solar irradiance happen on various timescales and the irradiance has a strong dependence on the various features present on the solar disk (Foukal et al. 2004; Fröhlich & Lean 2004). It has been found that the total solar irradiance is highly correlated with the fractional plage area or the plage index (Bertello et al. 2010). Recently, Bertello et al. (2016) found a strong correlation between the sunspot number and the Ca II K emission index. Thus the study of long-term plage data is important in connection not only with studies of the variation of the solar irradiation but also with the evolution of the solar magnetic field and its cyclic changes.

Various observatories around the globe have been taking routine observations of plages in the Ca II K line. The Mount Wilson data series is one such time series of the plage index (Bertello et al. 2010). Kodaikanal observatory in India obtained daily photoheliograms of the Sun from 1904 until 2007. This century-long data series has recently been digitized (Priyal et al. 2014). Chatterjee et al. (2016) used these digitized data to identify the plages using an automated algorithm and generated a plage area time series.

In this article, we use these data to find an association of the plages with sunspots. We also use these data to find different distributions in the plage sizes and their latitudinal locations.

2. Data Description

In this study we have used the plage area time series obtained from the newly digitized Kodaikanal Ca II K data. The complete time series covers more than 100 years of data (1904–2007). Due to issues with the conditions of the photographic plates and also a large number of days missing in the latter half of the data (see Figures 1(b) and 4 of Chatterjee et al. 2016), we chose to limit our analysis to the period between 1907 and 1965, which covers from cycle 14 (descending phase only) to cycle 19. For every detected plage form the daily Ca II K images, we have information on the heliographic latitude, longitude (in degrees), and area (in arcmin^2).

For the sunspot area data we have used the Greenwich daily sunspot record, for the same duration, available from the website https://solarscience.msfc.nasa.gov/greenwch.shtml.

3. Results

3.1. Yearly Averaged data and the Hemispheric Asymmetry

We generate the yearly averaged data from the daily plage observations and plot them (black solid line) in panel (a) of Figure 1 along with the sunspot area data (red solid line). Since we are interested in the association of the two structures, we plot the normalized values of the yearly averaged data. From the figure we readily see that the two time series show a good match with each other. Every feature, including the double peaks seen in the sunspot data, is also present in the plage area time series. To estimate this association quantitatively we plot the scatter diagram as shown in panel (b) of Figure 1. A correlation coefficient of 0.97 again confirms the close association of these two solar features, which have formed in two different layers in the solar atmosphere. However, we must emphasize that this high correlation in the

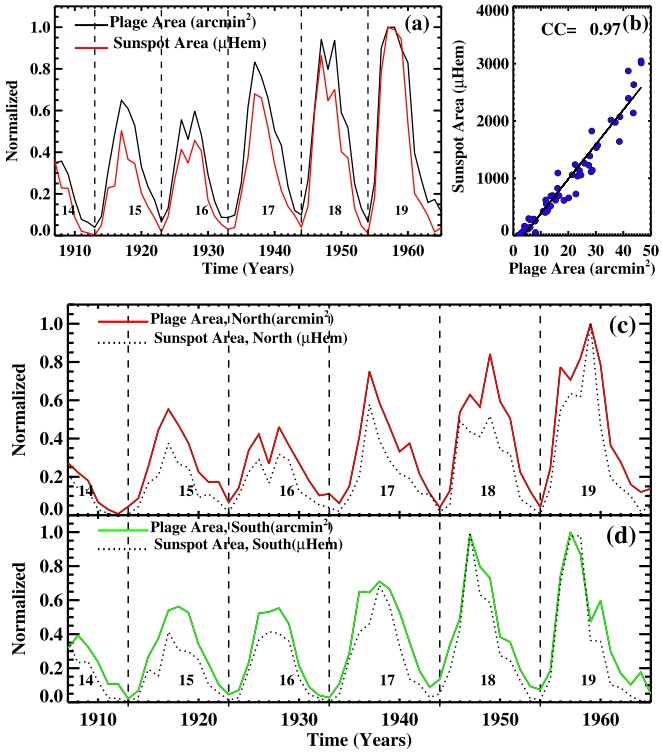

Figure 1. Panel (a) shows a comparison plot of the yearly averaged sunspot data and the plage area data. A scatter plot between the two sets of data is shown in panel (b). Panels (c) and (d) show the yearly averaged plage area in the northern and southern hemispheres as marked.

yearly data does not imply the same for shorter timescales (months or days). This is because when a sunspot decays away, the remnant small magnetic field may still continue to show itself as a plage in the higher atmosphere. Also, small-scale magnetic fields, which survive for a few days or less, do not always develop as a sunspot.

Now the hemispheric asymmetry in sunspot area is a well known phenomenon. We investigate the same from the plage area time series by computing the yearly data separately for the two hemispheres. Panels (c) and (d) in Figure 1 show the yearly averaged plage area data in the northern and southern hemispheres (plotted as red and green solid lines) respectively. The sunspot area data for the corresponding hemispheres are also plotted in the panels as black dotted lines. The hemispheric plage area series show a very good match with the sunspot area data. Similar to the sunspots, in this case too we find that the double peaks near the cycle maximum are not a persistent feature in both hemispheres. For example, the 16th cycle is double-peaked (see Figure 1(a)) but from Figures 1(c) and (d) we see that in this case only northern hemisphere shows a double-peak signature. In the case of the 19th cycle, no such double peak is seen in the overall case but both hemispheres have prominent double-peak signatures.

Next we compute the normalized asymmetry coefficient, defined as $(A_{\rm pn} - A_{\rm ps})/(A_{\rm pn} + A_{\rm ps})$, as a measure of the hemispheric asymmetry in the plage area ($A_{\rm pn}$ and $A_{\rm ps}$ are the yearly averaged values of plage area in the northern and southern hemispheres). The evolution of this asymmetry coefficient is plotted in panel (a) of Figure 2. There are quite a few distinct features readily noticeable from the plot. During the minima of cycles 14, 15, and 16, we see that the northern hemisphere dominates whereas for the later cycles, i.e., cycles 17–19, the

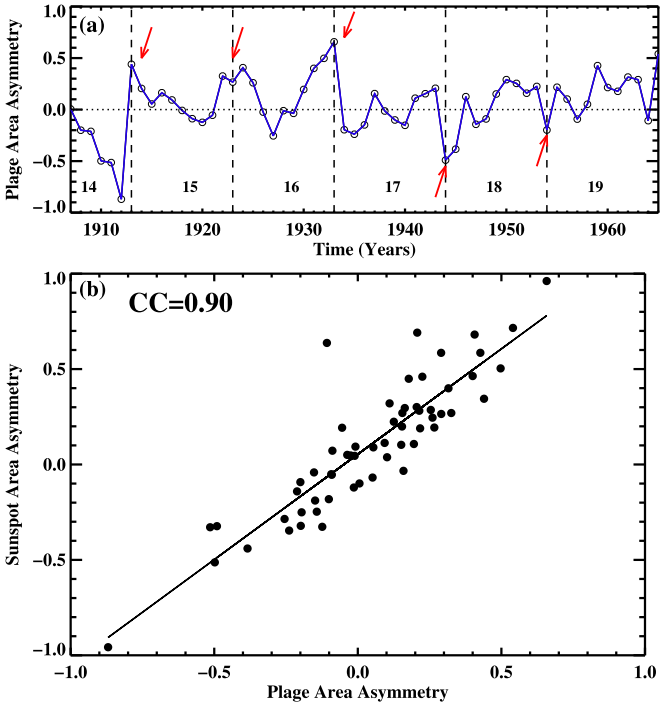

Figure 2. (a) Normalized plage area asymmetry. (b) Comparison of the same with the sunspot area asymmetry. The correlation value between these two is printed in the panel.

southern hemisphere dominates. This behavior is highlighted in the plot (Figure 2(a)) by using red arrows. It is also interesting to note that during the progression of a cycle the asymmetry coefficient changes its sign quite a few times, and this does not show any meaningful correlation with the cycle amplitude or any other property of that particular cycle. We also notice that on average the northern hemisphere dominates over the southern for the six cycles analyzed here. We revisit this dominance of the northern hemisphere in the following section.

Since we are interested in the plage–sunspot association, we look for the same in the asymmetry coefficient also. In panel (b) in Figure 2 we plot a scatter diagram between the asymmetry coefficients obtained from hemispheric plage area and the same computed for sunspot area. We find a very good match between these two coefficients with a correlation value of 0.90. However, we also found some outliers, which probably have occurred during the cycle minima, when the asymmetry coefficient is prone to large departures.

3.2. Plage Distributions

3.2.1. Size Distribution

Individual values of plage area are considered for the analysis of the size distribution. In panel (a) of Figure 3 we show the plage area (size) distribution for the whole time period, i.e., from 1907 to 1965. The distribution pattern looks similar to an exponentially decaying function. We fit the histogram with a decaying exponential function of the form, $Y = A_0 \exp^{-(\frac{X}{B})}$, as shown by the red dashed line in Figure 3(a). From the fit we notice that the initial part of the histogram is fit well but the fitted function drops very rapidly in the wing and leaves a large deviation around that region.

To get a better fit, we consider the log-normal function next. This is inspired by the fact the sunspots are known to have a

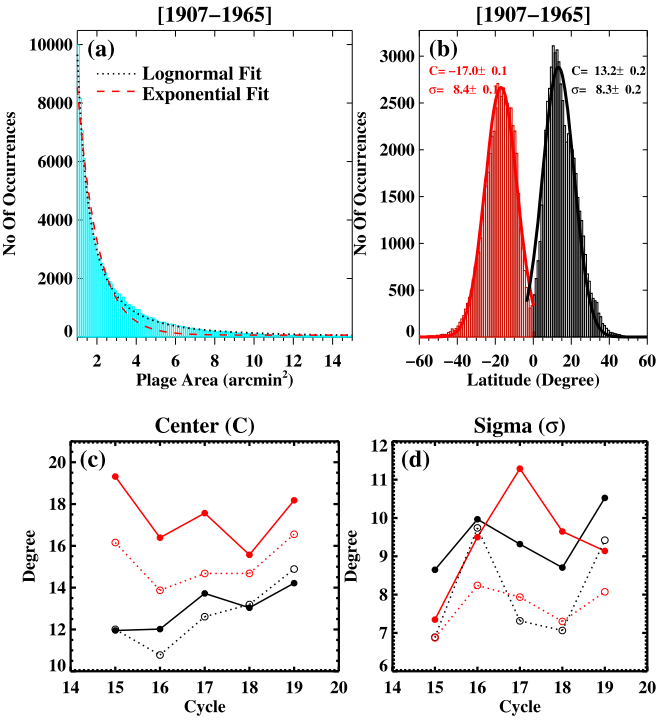

Figure 3. Panels (a) and (b) show the area and latitudinal distributions of the plages. Corresponding fits to these distributions are also overplotted in these panels. Panels (c) and (d) show (with solid black and red circles for the northern and southern hemispheres) the evolution of the fitted Gaussian parameters (C and σ) with the cycle number. We also overplot the same for the sunspots with open circles.

log-normal size distribution (Bogdan et al. 1988; Baumann & Solanki 2005; Mandal et al. 2017). Thus a log-normal function of the form

$$y = \frac{1}{\sqrt{2\pi}\,\sigma x}\exp\left(-\frac{[\ln(x) - \mu]^2}{2\sigma^2}\right)$$

is considered and fitted to the histogram as shown by the black dotted curve in Figure 3(a). In this case we notice that the full histogram along with the tail is fit very well. Thus the individual size distribution of the plages also follows the same "log-normal distribution" as we find for the sunspots. Here we must highlight the fact that the good match of the two functions (exponential and log-normal) at the core of the histogram (near to the origin, 1 arcmin^2) is due to the use of a rigid cutoff of 1 arcmin^2 as the minimum detectable plage area. Thus the initial increment of the log-normal distribution has been suppressed and the function decays exponentially thereafter.

3.2.2. Latitudinal Distribution

Plages occur at higher latitudes at the beginning of a cycle, and they move progressively toward the equator as the cycle progresses. We plot the distribution of the number of plages versus their latitudes, for the full time span (1907–1965), in panel (b) of Figure 3 (we also analyzed the same for the individual cycles). The plot shows two bell-shaped distributions corresponding to the two hemispheres, which are then fitted with two separate Gaussian functions. From this plot we notice that the peak height of the northern hemisphere is greater than that of southern hemisphere. This complements our findings in Section 3.1, where we obtained a similar result from analysis of the area asymmetry. To make a comparison, we repeat the same procedure for the Greenwich sunspot area data. From every Gaussian fit we note down two parameters: the center (C) and the sigma (σ) values. In panels (c) and (d) in Figure 3, we plot the evolution of these parameters for the plages and the sunspots simultaneously (solid red and black circles represent the values in the southern and northern hemispheres for the plages whereas the open circles corresponds to sunspots).

In the case of the center (C) plot (panel (c)) we see that the the centers of the plage distributions, for the two hemispheres, are always higher than those of the sunspots, although the trends remain the same. At the same time we notice that the differences is greater for the southern hemisphere. We also observe that the center of the southern hemisphere is higher for the 16th cycle than for the 19th cycle although the amplitude of the 19th cycle is much greater than that of the 16th cycle. In panel (d) we plot the evolution of the sigma parameter. Overall the evolution of this parameter for both indices, i.e., for sunspots and plages, follows the same pattern. Again we find that there is a noticeable difference in the southern hemisphere. The maximum sigma value occurs for the 17th cycle whereas for sunspots it occurs for the 16th cycle. Currently there is a very little theoretical understanding of the relation between these parameters and the solar dynamo. Recently Cameron & Schüssler (2016) found a connection between the parameter σ and the diffusivity (η) parameter used in the dynamo theory.

3.3. Correspondence between Plage and Sunspot Locations

Plages may be or may not be always associated with a sunspot for the reasons mentioned in Section 3.1. To investigate this, we divide the plages into four classes according to their individual sizes (A_p) and make use of the "butterfly diagram" for our further analysis. In different panels in Figure 4 we plot the time–latitude diagram for the individually detected plages with black circles whereas the green circles represent the locations of the sunspots. In the first size class (where $A_p \geqslant 1$ arcmin^2), we notice that there are a substantially large number of plages that do not have any sunspots associated with them. Also we notice that at the end of every cycle (or perhaps from the next cycle, due to the overlapping period) a large number of plages appear at high latitudes ($\approx 60^\circ$), and this is much more prominent in the southern hemisphere.

Now as we progressively go toward higher size thresholds ($A_p \geqslant 2$ arcmin^2, $A_p \geqslant 3$ arcmin^2, $A_p \geqslant 4$ arcmin^2) we see that the two butterfly diagrams (one for the sunspots and the other for the plages) show a progressively better match with each other. Thus, we conclude that the latitudinal locations of the plages with an area $\geqslant 4$ arcmin^2 show a very good match with the sunspot latitudes.

A latitudinal match does not necessarily imply a one-to-one correspondence between the two. This is because these features can be at same latitudes but at different longitudes, implying that the two are not connected at all. To better establish the association of plage sizes with the sunspot locations, we plot the longitudinal scatter diagrams for every plage size range as shown in the side panels in Figure 4. We record the area-weighted average longitudes for both the plages and the sunspots during simultaneous observing days. A careful analysis reveals that the scatter plots between the plage and sunspot longitudes become progressively more linear as we consider greater plage areas. Thus, in combination with our previous results from analysis of the "butterfly diagram," we

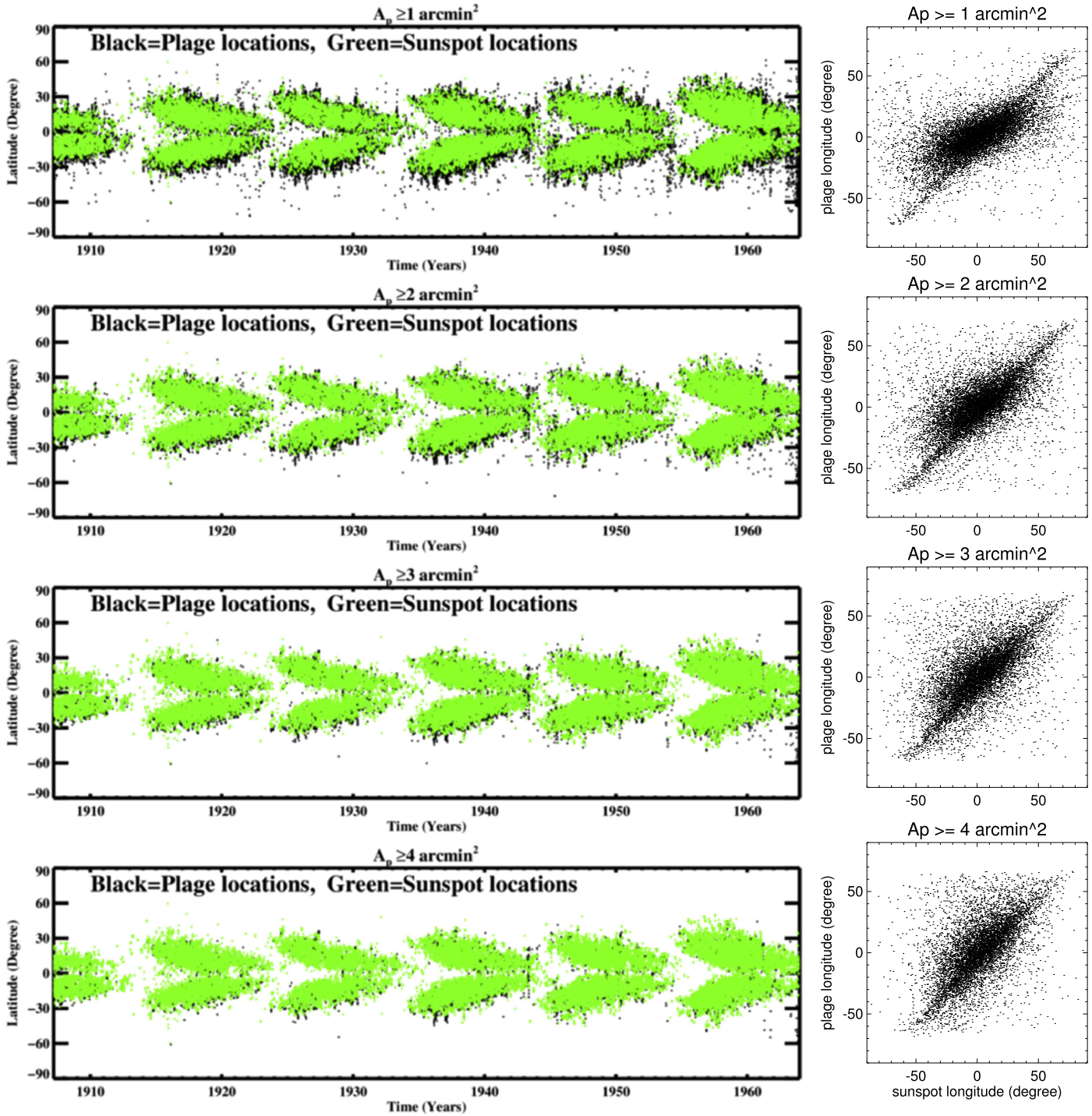

Figure 4. (Top to bottom) Comparison of the "butterfly diagram" for the plages (black circles) and the sunspots (green circles). The longitudinal scatter diagrams between the two are shown in the side panels. Different plage sizes (A_p) are mentioned in the title of the panels. An animated gif file of the above figure is available at ftp://ftp.iiap.res.in/dipu/plage_sunspot.gif.

conclude that plages with area $\geqslant$4 arcmin^2 have a better one-to-one correspondence with the sunspot locations. We must again remind the reader that the decay of a sunspot does not necessarily mean the disappearance of the associated plage.

3.4. Plage Sizes and the 11 Year Cycle

Various long-term and short-term properties of the sunspot cycle show a strong size dependence (Mandal & Banerjee 2016). Inspired by the findings of the dependence of plage size on the plage–sunspot association in the previous section, we look for different signatures in the cycle properties when the plages are considered according to their sizes. In panel (a) of Figure 5 we plot the "no thresholding" case, and in panels (b)–(d) we plot the yearly averaged variations in plage area for different size thresholds.

For the smallest plages (1 arcmin^2 $\leqslant A_p <$ 2 arcmin^2) we do not see much difference from the overall cycle characteristics

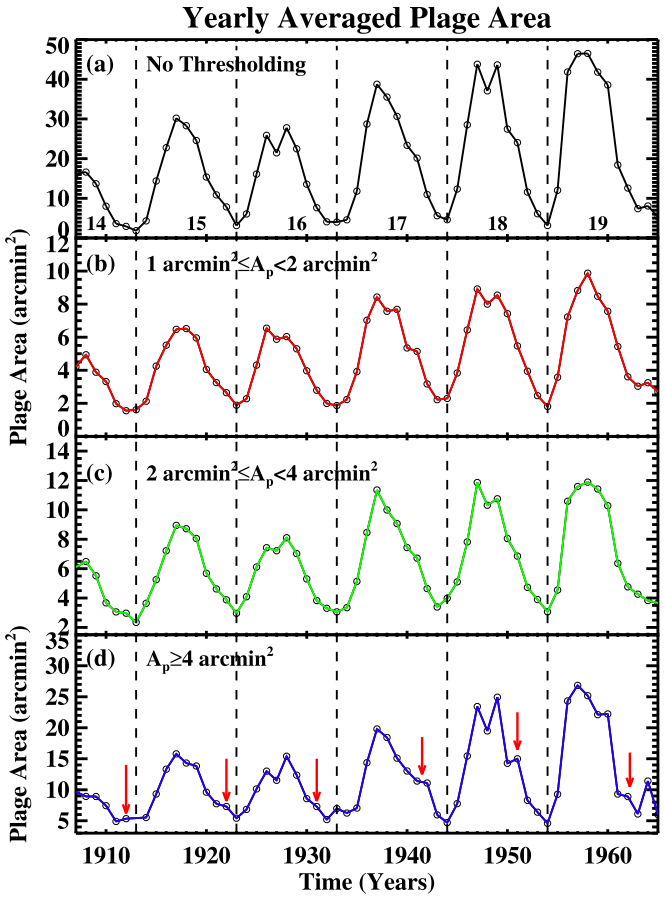

Figure 5. Different panels showing the time series of yearly averaged plage area as obtained using different plage size criteria. Individual size ranges are printed on each panel.

(as found in panel 5(a)), except for the double-peak behavior for certain cycles. For example, the double peaks of cycle 16 and cycle 18 become less prominent or weaker. Also the overall strength of the cycle does not change much for the smallest plage size range, i.e., the 19th cycle is still the strongest during the analyzed time span. The scenario almost remains the same for the medium plage size range (panel (c)). As we move toward the biggest plages (panel (d)), we notice that the double peaks near the cycle maxima appear for almost every cycle. This is consistent with the behavior of the biggest sunspots found by Mandal & Banerjee (2016). Apart from that we also note an interesting behavior, i.e., the presence of a weaker peak near the cycle minimum. This is highlighted in the panel by red arrows. The separation of this peak from the cycle maximum seems to reduce as we move from cycle 14 to cycle 19. This trend, however, is not prominently visible for the 19th cycle because we see a double peak late after the cycle maximum.

Next, we investigate the "odd–even rule" or the "G-O rule," which states that each odd-numbered cycle is stronger than the preceding even-numbered one (Gnevyshev & Ohl 1948). This is well established for the data on sunspot area and sunspot numbers. From Figure 5 we notice that this rule is also valid for plage area time series for all the size ranges. Still, it should be mentioned here that the relative heights of the cycles change slightly when one considers different size ranges (panels (b)–(d) of Figure 5).

4. Summary and Conclusion

A long-term multi-wavelength study of different solar features helps us to better understand the evolution of magnetic field in different layers of the solar atmosphere on different timescales. Sunspots and plages, though formed at different heights in the solar atmosphere, show a good correlation with each other at timescales comparable to the solar cycle. On shorter timescales of months or days, we find certain differences, though. Such differences can be explained by considering the complex evolution of the magnetic fields associated with sunspots. When a sunspot decays the fields get fragmented, and this process results in its disappearance from the white-light images. The remaining small-scale fields survive for quite a few days and continue to appear as plages in subsequent Ca II K images.

Analyzing the areas of the individual plages, we find that they follow a log-normal distribution similar to the sunspots. We also obtain a Gaussian distribution, in each hemisphere, of their latitudinal appearances. Some of the properties of the fitted Gaussian parameters show a different evolution with the solar cycle than the sunspots do. Though not well understood, this hints at a small-scale component of the solar dynamo that is responsible for the evolution of the small-scale fields. This aspect is explored further by implementing different size criteria on the individual plages and considering their time evolution. We find that different properties of the cycle change with the plage sizes, which again points toward a complex dynamo operating in the Sun. Finally we use the "butterfly diagram" along with longitudinal scatter plots to show that plages with sizes $\geqslant 4$ arcmin^2 are always associated with a sunspot.

To conclude, we have analyzed the newly digitized Ca II K data from Kodaikanal observatory to investigate the association of plages, a chromospheric structure, with sunspots, which are photospheric structures. For the first time, to our knowledge, individual plage sizes are considered and compared with the sunspot area data. Our analysis shows that the two layers (the chromosphere and photosphere) are magnetically coupled and that the dynamo responsible for the magnetic fields in the Sun may have a complex action (the generation of large-scale and small-scale fields).

We would like to thank the Kodaikanal facility of Indian Institute of Astrophysics, Bangalore, India for providing the data. These data are now available for public use at http://kso.iiap.res.in/data.

References

Baumann, I., & Solanki, S. K. 2005, A&A, 443, 1061
Bertello, L., Pevtsov, A., Tlatov, A., & Singh, J. 2016, SoPh, 291, 2967
Bertello, L., Ulrich, R. K., & Boyden, J. E. 2010, SoPh, 264, 31
Bogdan, T. J., Gilman, P. A., Lerche, I., & Howard, R. 1988, ApJ, 327, 451
Cameron, R. H., & Schüssler, M. 2016, A&A, 591, A46
Chatterjee, S., Banerjee, D., & Ravindra, B. 2016, ApJ, 827, 87
Foukal, P., Bernasconi, P., Eaton, H., & Rust, D. 2004, ApJL, 611, L57
Fröhlich, C., & Lean, J. 2004, A&ARv, 12, 273
Gnevyshev, M. N., & Ohl, A. I. 1948, AZh, 25, 18
Mandal, S., & Banerjee, D. 2016, ApJL, 830, L33
Mandal, S., Hegde, M., Samanta, T., et al. 2017, A&A, in press (arXiv:1608.04665)
Priyal, M., Singh, J., Ravindra, B., Priya, T. G., & Amareswari, K. 2014, SoPh, 289, 137
Sheeley, N. R., Jr., Cooper, T. J., & Anderson, J. R. L. 2011, ApJ, 730, 51